OMTM, Volume *17*

Supplemental Information

DNAJC14 Ameliorates Inner Ear Degeneration in the DFNB4 Mouse Model

Hye Ji Choi, Hyun Jae Lee, Jin Young Choi, Ik Hyun Jeon, Byunghwa Noh, Sushil Devkota, Han-Woong Lee, Seong Kug Eo, Jae Young Choi, Min Goo Lee, and Jinsei Jung

Supplementary Table S1. Antibodies used in this study.

Name	Catalog number (Manufacturer)	Dilution (Use)
Primary Antibody		
Pendrin	G-19 (Santa Cruz)	1:1000 (WB)
Aldolase	N-15 (Santa Cruz)	1:1000 (WB)
3xHA-DNAJC14	F-7 (Santa Cruz)	1:1000 (WB)
Myc-Hsc70	1B5 (Abcam)	1:1000 (WB)
HA-Arf1	F-7 (Santa Cruz)	1:1000 (WB)
anti-pendrin	2-hR2 (ABfrontier)	1:1000 (WB)
anti-β-Actin	sc-47778 (Santa Cruz)	1:2000 (WB)
anti-DNAJC14	ab121535 (Abcam)	1:1000 (WB), 1:200 (IF)
anti-Flag	F3165 (Sigma)	1:2000 (WB), 1:100 (IF)
anti-DAPI	D1306 (Thermo)	1:5000 (ICC), 1:10000 (IHC)
anti-KCNJ10	APC-035 (Alomone Labs)	1:100 (IF)
Secondary Antibody		
anti-mouse, HRP conjugated	G-21040 (Thermo)	1:1000 (WB)
anti-rabbit, HRP conjugated	32460 (Thermo)	1:1000 (WB)
Alexa 488, anti-mouse	A11001 (Invitrogen)	1:1000 (IF)
Alexa 488, anti-rabbit	A11008 (Invitrogen)	1:1000 (IF)
Alexa 568, anti-rabbit	A11036 (Invitrogen)	1:1000 (IF)

IF, immunofluorescence; WB, western blotting; IHC, immunohistochemistry; ICC, immunocytochemistry

Figure S1

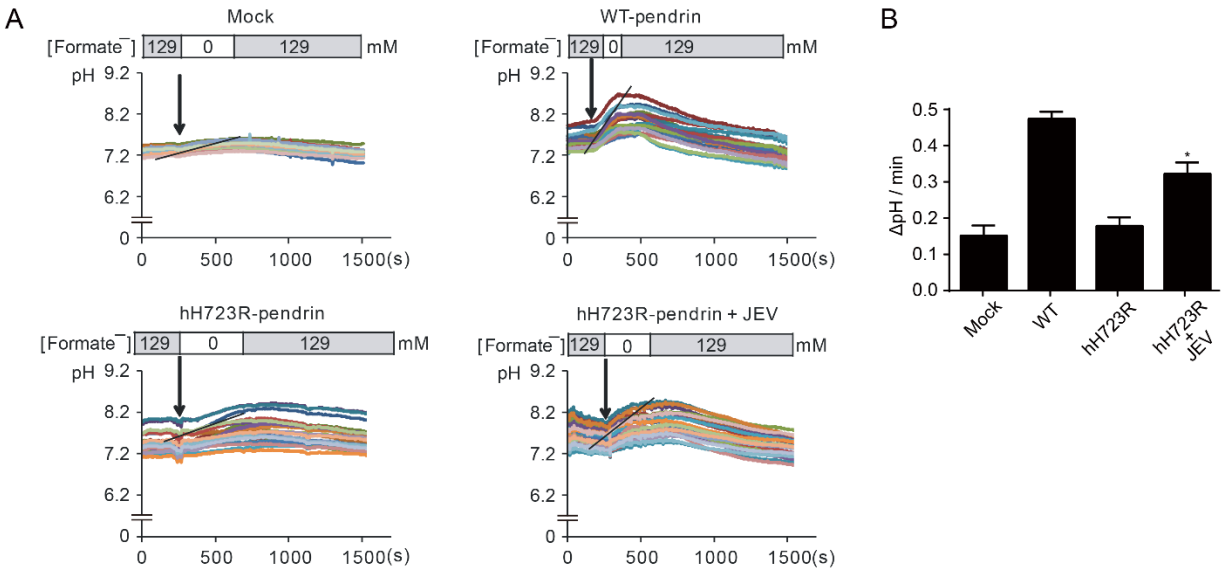

Figure S1. HCO_2^-/HCO_3^- exchange activity by activation of DNAJC14. (A) Formate/Bicarbonate (HCO_2^-/HCO_3^-) exchange activity was measured by recording the pH-sensitive fluorescent probe BCECF in PANC-1 mock cells, and in wild-type (WT)- and human H723R (hH723R)-pendrin stably expressing cells with/without Japanese encephalitis virus (JEV, $3x10^6$ pfu) to activate DNAJC14, as detailed in the Methods. The quantification of multiple experiments is depicted in (B). The HCO_2^-/HCO_3^- exchange activity significantly increased in cells expressing hH723R-pendrin with JEV treatment (n = 4 in each group). *, $p < 0.05$.

Figure S2

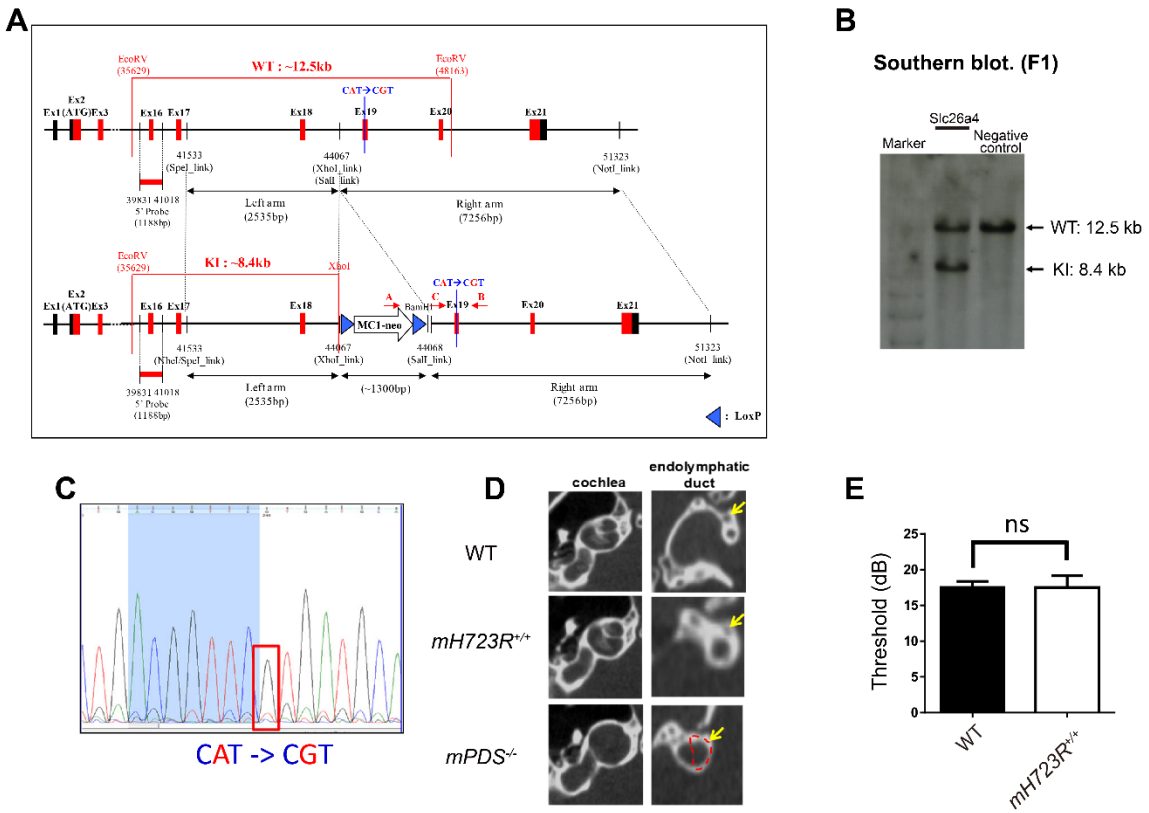

Figure S2. Targeting scheme of the H723R knock-in mouse model. (A) A Bac clone containing *slc26a4* genomic region was used to construct the targeting vector. The expected size of the restriction enzyme fragment of the wild-type (WT) and knock-in (KI) was ~12.5 kb and ~8.4 kb, respectively. The loxP-flanked neomycin resistance gene (neo) was used as a selection marker during embryonic stem (ES) cell culture. (B) The *slc26a4* knock-in (KI) was identified with Southern blotting. (C) Sanger sequencing of the target region revealed that the c.2168A>G point mutation was present in the founder mouse. (D) Micro-computed tomogram of the inner ear. While *slc26a4* knock-out mice (*mPDS*$^{-/-}$) showed a dilated endolymphatic duct and cochlear hydrops, WT and mouse p.H723R KI homozygote [*mH723R*$^{+/+}$] showed normal cochlea and endolymphatic duct. (E) In the auditory brainstem response, both WT and *mH723R*$^{+/+}$ mice showed normal hearing thresholds (n = 13 in each group). ns, not significant.

Figure S3

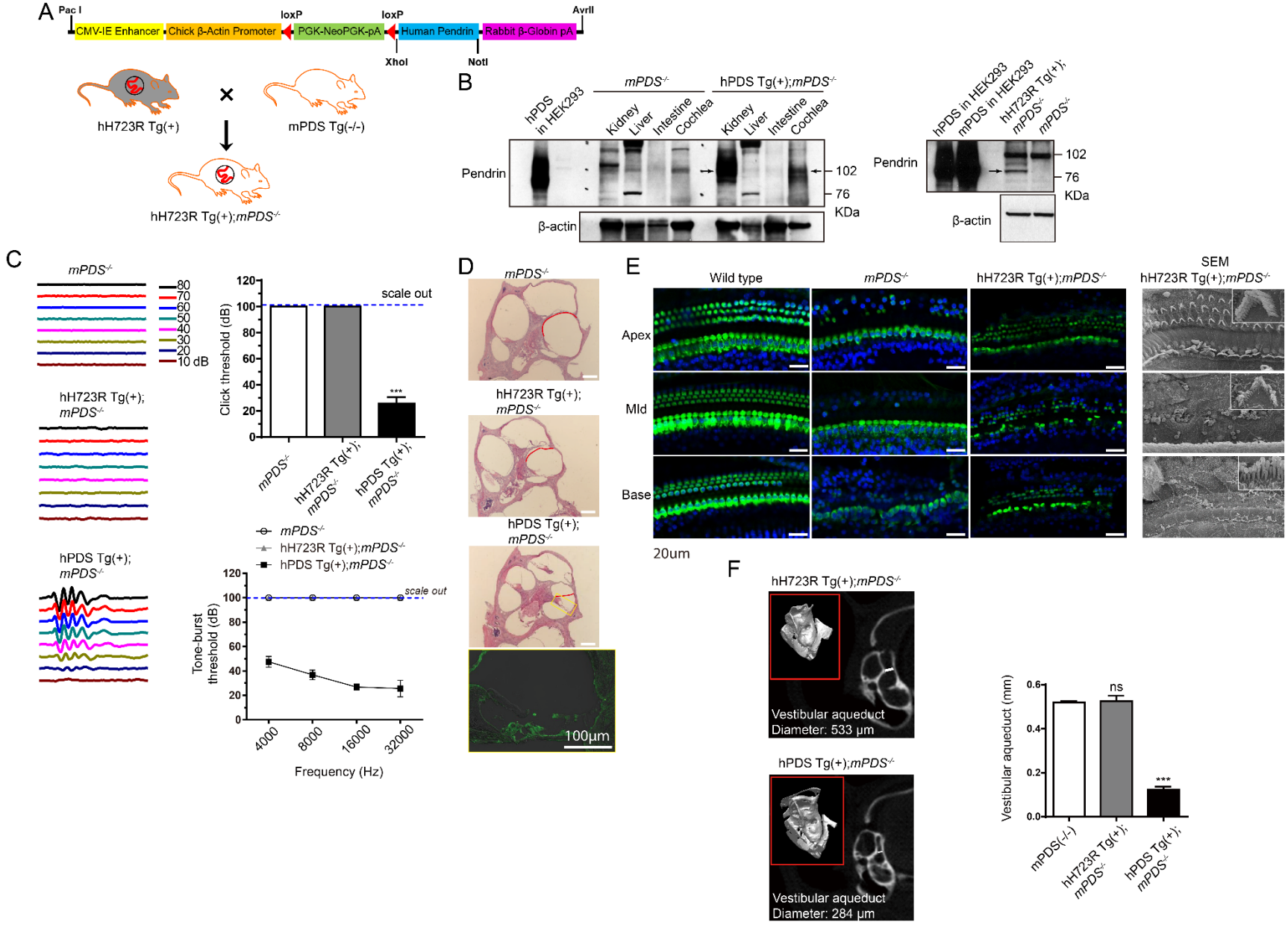
A
Pac I
loxP
loxP
AvrII
CMV-IE Enhancer
Chick β-Actin Promoter
PGK-NeoPGK-pA
Human Pendrin
Rabbit β-Globin pA
XhoI
NotI
hH723R Tg(+)
mPDS Tg(-/-)
hH723R Tg(+);mPDS-/-
B
hPDS in HEK293
mPDS-/-
hPDS Tg(+);mPDS-/-
Kidney
Liver
Intestine
Cochlea
Pendrin
β-actin
102
76
KDa
hPDS in HEK293
mPDS in HEK293
hH723R Tg(+); mPDS-/-
mPDS-/-
C
mPDS-/-
80
70
60
50
40
30
20
10 dB
hH723R Tg(+); mPDS-/-
hPDS Tg(+); mPDS-/-
Click threshold (dB)
scale out
***
mPDS-/-
hH723R Tg(+); mPDS-/-
hPDS Tg(+); mPDS-/-
mPDS-/-
hH723R Tg(+);mPDS-/-
hPDS Tg(+);mPDS-/-
Tone-burst threshold (dB)
scale out
4000
8000
16000
32000
Frequency (Hz)
D
mPDS-/-
hH723R Tg(+); mPDS-/-
hPDS Tg(+); mPDS-/-
100μm
E
Wild type
mPDS-/-
hH723R Tg(+);mPDS-/-
SEM
hH723R Tg(+);mPDS-/-
Apex
Mid
Base
20um
F
hH723R Tg(+);mPDS-/-
Vestibular aqueduct
Diameter: 533 μm
hPDS Tg(+);mPDS-/-
Vestibular aqueduct
Diameter: 284 μm
Vestibular aqueduct (mm)
ns
***
mPDS(-/-)
hH723R Tg(+); mPDS-/-
hPDS Tg(+); mPDS-/-

Figure S3. Generation of a human H723R-pendrin mouse model mimicking deafness in human DFNB4.

(A) Construct of the human p.H723R *SLC26A4* transgene in the pCB vector backbone. The wild-type (WT) or the p.H723R *SLC26A4* gene is Cre-inducible. The human WT-pendrin (hPDS) and H723R-pendrin (hH723R) transgenic mice [Tg(+)] were crossed with pendrin knock-out [$mPDS^{-/-}$] mice to generate hH723R Tg(+);$mPDS^{-/-}$ mice, in which only ectopic hH723R-pendrin was expressed without expression of mouse pendrin. To induce transgene expression in the inner ear, we crossed this strain with Pax2-Cre mice. (B) When WT- or hH723R-Tg(+) mice were crossed with Pax2-Cre, expression of the *SLC26A4* gene was observed in the inner ear and kidney (black arrows), but not in the other organs. (C) Auditory brainstem response by click and tone-burst stimuli for $mPDS^{-/-}$, hH723R(+);$mPDS^{-/-}$, and hPDS Tg(+);$mPDS^{-/-}$ mice. $mPDS^{-/-}$ and hH723R Tg(+);$mPDS^{-/-}$ mice were deaf, whereas the hearing function of hPDS Tg(+);$mPDS^{-/-}$ mice was nearly normalized (n = 8 mice in each group). (D) H&E staining of the inner ear showing that mPDS(−/−) and hH723R Tg(+);$mPDS^{-/-}$ mice had dilatation of the scala media, whereas hPDS Tg(+);$mPDS^{-/-}$ mice had normal sized scala media without endolymphatic hydrops. Immunostaining of the inner ear (lower panel) showed ectopic pendrin expression (anti-pendrin antibody, green) in the hair cells, supporting cells, inner limbus, lateral wall, and stria vascularis (Pax2-Cre-dependent). Scale bar, 20 μm. (E) Immunofluorescence and surface electron microscopy (SEM) images of the organ of Corti labeled with phalloidin (green) and DAPI (blue) in wild-type, $mPDS^{-/-}$, and hH723R Tg(+);$mPDS^{-/-}$ mice. Note that the outer hair cells showed better survival in hH723R Tg(+);$mPDS^{-/-}$ than in $mPDS^{-/-}$ mice. Magnification of electron microscope is x2000 [inset: x30000 (upper and middle), and x35000 (lower)). Scale bars, 20 μm. (F) Micro-computed tomogram was performed to compare the size of vestibular aqueduct. hH723R Tg(+);$mPDS^{-/-}$ mice had enlarged vestibular aqueduct, which was comparable to $mPDS^{-/-}$ mice. In contrast, hPDS Tg (+);$mPDS^{-/-}$ showed significantly normalized size of vestibular aqueduct when compared to that of $mPDS^{-/-}$ (n = 6–9 in each group). ns, not significant; ***, $p < 0.001$.